Research Paper

Sub-stoichiometric titanium oxide as a new anode material for electro-Fenton process: Application to electrocatalytic destruction of antibiotic amoxicillin

Nihal Oturan[a], Soliu O. Ganiyu[a], Stephane Raffy[b], Mehmet A. Oturan[a],*

[a] Université Paris-Est, Laboratoire Géomatériaux et Environnement (EA 4508), UPEM, 77454 Marne-la-Vallée, France
[b] Saint-Gobain C.R.E.E., 550 avenue Alphonse Jauffret, 84300 Cavaillon, France

ABSTRACT

This study report, for the first time, the potential use of sub-stoichiometric titanium oxide (Ti_4O_7) elaborated by plasma deposition, as an efficient, stable and cost-effective anode material for electrocatalytic oxidation of organic pollutants by electro-Fenton process. The antibiotic amoxicillin (AMX) was selected as target pollutant and the oxidative degradation of this drug was ensured by hydroxyl radicals generated both at Ti_4O_7 surface by oxidation of water and in the bulk solution from electrocatalytically produced Fenton's reagent. A quick oxidation of 0.1 mM (36.5 mg L^{-1}) AMX was obtained in a short electrolysis time for all applied current studied while its almost complete mineralization was attained even at a low current intensity of 120 mA. The performance of this new anode material in term of degradation kinetics, mineralization current efficiency (MCE) and energy cost was compared with boron doped diamond (BDD) and other conventional anodes such as platinum (Pt) and dimensional stable anode (DSA). Results showed that Ti_4O_7 provides similar oxidation rate and MCE as BDD at all current studies, while it give significantly better results than DSA and Pt anodes. The solutions treated by electro-Fenton process using Ti_4O_7 anode showed low percentage bioluminescence inhibition to *V. fischeri* bacteria, indicating excellent detoxification of the AMX solution. Therefore, Ti_4O_7 anode appears to be an interesting cost-effective alternative anode material to BDD and other industrial electrodes for electro-Fenton processes since its production is very inexpensive when compared to BDD.

© 2017 Elsevier B.V. All rights reserved.

1. Introduction

Electro-Fenton (EF) oxidation is one of the most prominent and efficient advanced oxidation processes (AOPs) that have been widely studied for the removal of toxic/persistent organic pollutants (POPs). It involves the formation of hydroxyl radicals ($^\bullet$OH) in the bulk via Fenton's reaction (Eq. (2)) between continuously electrogenerated H_2O_2 at a suitable cathode (Eq. (1)) fed with air/O_2 and iron catalyst initially added to the treated solution at catalytic quantities [1–6]. Interestingly the catalyst (Fe^{2+}) consumed in reaction (2) is electrocatalytically regenerated in reaction (3).

$$O_2 + 2H^+ + 2e^- \rightarrow H_2O_2 \tag{1}$$

$$H_2O_2 + Fe^{2+} \rightarrow Fe^{3+} + OH^- + {}^\bullet OH \tag{2}$$

$$Fe^{3+} + e^- \rightarrow Fe^{2+} \tag{3}$$

Although the oxidation of the pollutants in EF process occurs primarily in the bulk, thanks to the large amount of homogeneously generated hydroxyl radicals ($^\bullet$OH) via electrocatalytically generated Fenton's reagent, the nature of the anode material (M) plays also a significant role on the process efficiency due to the generation of heterogeneous hydroxyl radical M($^\bullet$OH) (Eq. (4)) which contributes to the overall oxidation/mineralization of the organic pollutants. This is particularly the case of non-active anodes such as BDD or PbO_2 with large O_2 evolution overvoltage [7–13]. Several studies have shown that M($^\bullet$OH) is more efficient in oxidation of highly recalcitrant short-chain carboxylic acids, which are the ultimate intermediate products before complete mineralization of organics by AOPs, whereas $^\bullet$OH produced in the bulk is relatively less reactive toward this species [[14–18]]. Therefore, the nature of anode material is an important parameter in EF process for an efficient treatment of persistent/toxic organic pollutants.

$$M + H_2O \rightarrow M({}^\bullet OH) + H^+ + e^- \tag{4}$$

* Corresponding author.
  E-mail addresses: Mehmet.oturan@univ-paris-Est.fr, mehmet.oturan@u-pem.fr (M.A. Oturan).

Many authors have reported partial mineralization of organics by EF process when "active" anodes like Pt and DSA, that have lower O_2 evolution overpotential, are utilized as anode materials due to the chemisorption of the generated $M(^\bullet OH)$ on anode surface making them less efficient in mineralization of recalcitrant organics [8,19–23]. In contrast, almost complete mineralization has been achieved in EF oxidation of persistent organics with non-active anode like BDD [3,24–28] for which $M(^\bullet OH)$ is more available due to its physisorption. All these reports pointed out that the efficiency of EF process can be significantly enhanced by using a non-active anode such as BDD. However, BDD anode is highly expensive and currently not economically viable on industrial scale [11,29]. Other available non-active anodes such as doped PbO_2 and SnO_2 have never been utilized in EF process due to their stability and the likely leaching of toxic ions to treated solution.

Magnéli phase ceramic electrodes based on sub-stoichiometric titanium oxides with generic formula Ti_nO_{2n-1} ($3 \leq n \leq 9$) were developed in early '80s, but recently investigated as low cost alternative electrode materials in electrochemical water treatment because they are produced from TiO_2, one of the most abundant feedstocks available on the planet [30–32]. Several oxides in this series, especially Ti_4O_7 exhibits high electrical conductivity at room temperature, good corrosion resistant and high chemical stability even in extremely corrosive media [33–36]. Generally Ti_4O_7 can be prepared by annealing Ti film in oxygen environment [32] or reducing TiO_2 by using carbon [33], H_2 [37], NH_3 [38], N_2 [39], Zr [40], and spark plasma sintering [41]. Studies have shown that this electrode behaves as non-active anode, i.e., generates weekly sorbed $^\bullet OH$ on its surface, that can lead to the electrochemical combustion of organics to CO_2 [32,42,43]. Some authors, including our group, have studied the potential of this anode material at low currents in anodic oxidation of organic pollutants [44–46], but no study available in literature on application of this anode material in EF process.

In this context we investigated for the first time, the use of Ti_4O_7 as a suitable anode material for EF process. Ti_4O_7 films can be manufactured by plasma coating, which is a widely spread technology, largely used for many types of applications (corrosion protection, abrasion resistance, thermal barriers, etc.). It was prepared by two step technique: (i) reduction of TiO_2 with coke to produce Ti_xO_{2x-1} powder and (ii) plasma elaboration of Ti_xO_{2x-1} on Ti-alloy substrate at 10 000–15 000 °C accompanied by conversion of all sub-oxides of Ti to Ti_4O_7 [46]. Plasma coating technology makes it possible to coat large surfaces, up to 1 m^2 or even larger, which is a definite advantage and cost-reducing technique for commercial production of electrodes compared to the chemical vapor deposition technology used in fabrication of BDD anodes. Therefore we investigated the ability of this anode for oxidation of a common antibiotic, amoxicillin (AMX), which was used as target pollutant and to the mineralization of its aqueous solution. Comparative experiments were carried out with anode materials such as BDD, Pt and DSA under same operating conditions. Moreover, the energy consumption of EF process related to each anode material as well as evolution of the acute toxicity during the treatment were assessed.

2. Materials and methods

2.1. Chemicals

AMX ($C_{16}H_{19}N_3O_5S$), sodium sulfate (Na_2SO_4), iron (II) sulfate heptahydrate ($FeSO_4 \cdot 7H_2O$) were obtained from Sigma-Aldrich. Sulfuric acid (H_2SO_4) and sodium hydroxide (NaOH) used to adjust solution pH were of analytical grade from Acros Organics and Fluka. Oxalic ($H_2C_2O_4$), oxamic ($C_2H_3NO_3$), acetic ($C_2H_4O_2$), maleic ($C_4H_4O_4$), glycoxylic ($C_2H_2O_3$) and malonic ($C_3H_4O_4$) acids used

as standards for quantifying short-chain aliphatic carboxylic acids generated during EF treatment were obtained from Acros, Fluka and Alfa Aesar. Bioluminescent bacteria *Vibrio fischeri* and the activation reagent LCK 487 LUMISTOX were supplied by Hach Lange France SAS. Organic solvents and other chemicals used were either HPLC or analytic grade from Sigma-Aldrich, Fluka and Merck. All solutions were prepared with ultra-pure water obtained from a Millipore Milli-Q system with resistivity>18 MΩ cm at 25 °C.

2.2. Electrochemical cell

The electrolyses were performed in a 250 mL undivided cylindrical glass cell equipped with two electrodes and stirred with PTFE magnetic bar. The anode was an electrode of 24 cm^2 surface area (4 cm × 6 cm) made of either Ti_4O_7 thin film plasma deposited on Ti alloy, Saint Gobain C.R.E.E., France), commercial pure Pt mesh, commercial DSA ($RuO_2–IrO_2$ thin film deposited on Ti, Baoji Xinyu GuangJiDian Limited Liability Company, China) or BDD (thin film deposited on Nb support, Condias Gmbh, Germany), while the cathode was a tri-dimensional, large surface area (14 cm × 5 cm × 0.5 cm) carbon-felt (CF) (MERSEN, France). The anode was always centered in the electrochemical cell, surrounded by the CF cathode. Compressed air was continuously bubbled into the cell at about 1 L min^{-1} to ensure an O_2 saturated solution. 230 mL aqueous solutions of 0.1 mM AMX (19.6 mg L^{-1} TOC) containing 0.05 M Na_2SO_4 as supporting electrolyte and 0.1 mM Fe^{2+} (catalyst) were used to conduct the electrochemical experiments at pH 3 and applied current in the range of 10–120 mA. All trials for kinetics measurements and TOC decay of solutions were conducted at room temperature (23 ± 2 °C) and made in triplicate. The average values with an error <2% are reported on the figures.

2.3. Analytical procedures

Electrolyses were performed with a Hameg HM7042-5 triple power supply at constant current. The total organic carbon (TOC) removal was monitored by Shimadzu VCSH TOC analyzer using the non-purgeable organic carbon method with ± 2% accuracy. The data obtained were used to estimate the mineralization degree of treated AMX solution and the mineralization current efficiency (MCE) (using Eq. (5)) for each treated solution at a given electrolysis time based on complete electrochemical oxidation of AMX (Eq. (6)) [14,47].

$$MCE(100\%) = \frac{nFV_s \Delta(TOC)_{exp}}{4.32 \times 10^7 mIt} \times 100 \qquad (5)$$

where F is the Faraday constant (96487C mol^{-1}), V_s is the solution volume (L), 4.32×10^7 is a conversion factor (=3600 s h^{-1} × 12,000 mg of C mol^{-1}), m is the number of carbon atoms of AMX (16C atoms), I is the applied current (A) and n is the number of electron consumed per molecule of AMX; taken to be 94 assuming complete mineralization of AMX into CO_2, NO_3^- and SO_4^{2-} according to Eq. (6).

$$C_{16}H_{19}N_3O_5S + 40H_2O \rightarrow 16CO_2 + 3NO_3^- + SO_4^{2-} + 99H^+ + 94e^- \qquad (6)$$
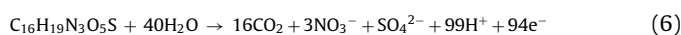
The decay of concentration of AMX was followed by uHPLC (Thermo Scientific) model "Ultimate 3000" equipped with a DAD detector and a RP-18 Hypersil 1.9 μm (10 cm × 2.1 mm) column eluted with water/methanol/acetic acid 92:6:2 at flow rate of 0.2 mL min^{-1}. Short-chain carboxylic acids generated during the EF treatment were identified and quantified by ion-exclusion HPLC using Merck Lachrom liquid chromatograph equipped with a L-2130 pump fitted with a C18 Acclaim OA, 4 mm × 25 cm (i.d.) column at 40 °C, and coupled with a L-2400 UV detector selected at wavelength of 210 nm, using 1% H_2SO_4 at 0.2 mL min^{-1} as mobile phase. NH_4^+, NO_3^{---} and SO_4^{2---} ions released into electrolyzed

Table 1
Apparent rate constant ($k_{app(AMX)}$) (min^{-1}) values for the oxidation of AMX by $^{\bullet}OH/M(^{\bullet}OH)$ generated in EF process with Ti_4O_7, BDD, DSA and Pt anodes, assuming pseudo-first order reaction kinetics.

I (mA)			$k_{app(AMX)}$	
Anode	10	30	60	120
Ti_4O_7	0.09	0.20	0.35	0.62
BDD	0.09	0.20	0.31	0.62
DSA	0.06	0.16	0.24	0.52
Pt	0.06	0.19	0.30	0.61

solutions were identified and quantified by Dionex ICS-1000 Basic Ion Chromatography set-up coupled with a Dionex DS6 conductivity detector containing a cell maintained at 35 °C and monitored through Chromeleon SE software. The NH_4^+ content was quantified by a Dionex CS12A, 25 cm × 4 mm (i.d.) cation column and a mobile phase of 9 mM H_2SO_4 at 1.0 mL min^{-1}, whereas the content of NO_3^{---} and SO_4^{2---} ions was measured with a Dionex AS4A-SC, 25 cm × 4 mm (i.d.) anion-exchange column using a mixture of 1.8 mM Na_2CO_3 and 1.7 mM $NaHCO_3$ solution at 2.0 mL min^{-1} as mobile phase.

Evolution of solution toxicity during EF treatment was monitored by Microtox® method [48,49]. The inhibition of the bio-luminescence of the bacteria *V. fischeri* was used to evaluate the toxicity of the electrolyzed samples. Prior to Microtox analysis, the pH of all the samples was adjusted to 6.5–7.5 with the aid of 0.01–0.1 mM NaOH solution. Bioluminescence measurements were performed on both blank as well as electrolyzed AMX solutions after 5 and 15 min of exposure to *V. fischeri* bacteria.

3. Results and discussion

3.1. Comparative degradation kinetics of AMX

A previous study showed that direct electron transfer process is negligible in the case of AMX and its oxidation can be mainly attributed to hydroxyl radicals [9]. Therefore results obtained during electro-Fenton treatment of AMX solutions were assessed in this context.

Fig. 1 illustrates the fast decay of AMX concentration obtained during the EF treatment for different anode materials under study. Similar and slightly faster degradation of AMX was observed with both Ti_4O_7 and BDD anodes compared to DSA and Pt anodes (see also Table 1). For example, the complete degradation of AMX required almost same electrolysis time as a function of applied current. This indicates that both anodes have quite similar oxidation power for degradation of AMX under same experimental conditions. This means that oxidation of AMX was carried out mainly in the solution by homogeneous $^{\bullet}OH$ produced in the bulk via electrochemically induced Fenton's reaction (Eq. (2)) through electrogeneration of H_2O_2 from 2-electron reduction of dissolved O_2 (Eq. (1)) and regeneration of Fe^{2+} (catalyst) from reduction of Fe^{3+} (Eq. (3)) produced by Fenton's reaction. On the other hand, a slightly longer time was required for complete removal of AMX when either DSA or Pt anode was used (Fig. 1d and c). The relatively slow degradation kinetics observed with DSA and Pt anodes can be explained by their lower ability to generate $M(^{\bullet}OH)$ compared to Ti_4O_7 and BDD anodes due to their lower O_2-evolution overpotential and chemisorption of produced radicals. This is because at similar experimental conditions, similar quantities of homogeneous hydroxyl radical are generated in the bulk of the solution by Fenton's reaction irrespective of anode material used. As such, the difference in degradation capacity observed was related to the quantities and potency of oxidant produced at the surface of the anode. In the case of Ti_4O_7 and BDD anodes, large quantities of heterogeneous hydroxyl radical are produced at the anode surface due

to their high O_2 evolution overpotential and their adsorption characteristics (physisorption). Unlike BDD and Ti_4O_7 anodes, Pt and DSA are active anodes with low O_2 formation overpotential leading to the formation of relatively lesser amount of $M(^{\bullet}OH)$ that are chemisorbed and consequently less available. Further, the results of Fig. 1 also show an increase in the oxidation rate of AMX as current rises from 10 to 120 mA with all the anodes, leading to a gradual shorter time for its total disappearance with increased applied current. This is expected because of the accelerated production of more $^{\bullet}OH$ in the bulk as well as more $M(^{\bullet}OH)$ at the anode surface [2,50–52] since the rate of hydroxyl radical production through reactions (Eq. (1)), (Eq. (3)) and consequently (Eq. (2)) as well as reaction (Eq. (4)) is monitored by applied current as the main operating parameter.

The decay of AMX concentrations (Fig. 1) was well fitted to pseudo-first order reaction kinetics, with excellent correlation ($R^2 \geq 0.99$), as depicted in the kinetic analysis shown in the inset panels. The corresponding apparent rate constants ($k_{app(AMX)}$) calculated from the slope of $ln(C_0/C_t)$ versus time plot (inset panels of Fig. 1) are given in Table 1. As expected, the $k_{app(AMX)}$ increased as applied current rose and interestingly the $k_{app(AMX)}$ values obtained for both Ti_4O_7 and BDD anodes were quite similar for all the applied currents studied, which is in agreement with our early assertion that both anode materials have very similar oxidation power for the degradation of AMX by EF process. Besides, the $k_{app(AMX)}$ values obtained for Pt anode was quite similar to the values obtained for both Ti_4O_7 and BDD anodes. However, lower $k_{app(AMX)}$ values was obtained with DSA anode, indicating its relatively lower oxidation potential compared to other anode materials studied. The effect of $M(^{\bullet}OH)$ on the oxidation of AMX remained almost negligible at shorter electrolysis times.

3.2. Mineralization of AMX by EF process with Ti_4O_7 in comparison with other anodes

The TOC abatement (as a measure of mineralization ability) with electrolysis time for the mineralization of 0.1 mM AMX (corresponding to initial TOC of 19.6 mg L^{-1}) solution is shown in Fig. 2. As can be seen in Fig. 2a and b, TOC was removed at similar rate for both Ti_4O_7 and BDD anodes at same operating conditions. In fact, the difference in TOC removal degree during EF treatment with Ti_4O_7 and BDD anodes after 6 h of electrolysis at all studied current was less than 1.5% (Fig. 2e), indicating that both anodes have similar oxidation potential. For instance, TOC removal efficiency of 89 and 90% were obtained for Ti_4O_7 and BDD anodes, respectively, after 6 h of electrolysis at 120 mA applied current. On the contrary, the comparison with other commercially available anodes like DSA and Pt, highlighted that this anode provides significantly better mineralization efficiency than DSA and Pt anodes at all applied current studied (Fig. 2c, d and f). For example after 6 h of electrolysis, the TOC removal efficiency of 34, 53, 69, and 74% were obtained at 10, 30, 60 and 120 mA respectively, with DSA anode, while 38, 60, 76, and 81% were obtained at similar applied currents with Pt (Fig. 2f) anode, whereas higher TOC removal of 50, 77, 84 and 89% were attained with Ti_4O_7 anode at the stated applied current. The higher mineralization degree obtained with Ti_4O_7 anode at all current studied compared to DSA or Pt could be explained by large generation of weakly adsorbed $Ti_4O_7(^{\bullet}OH)$ at the Ti_4O_7 anode surface, which can readily react with AMX and its intermediates, thus enhanced both oxidation and mineralization efficiency of the process. Contrarily, the generated $DSA(^{\bullet}OH)$ and $Pt(^{\bullet}OH)$ are chemisorbed on the anode surface, therefore less available for mineralization of organics [2,3,7]. As expected, the TOC removal kinetics enhances with rise of applied current for all anode materials studied due to the concomitant generation of more amount of $^{\bullet}OH$ in the bulk as well as at the more M(OH) at the surface of anodes
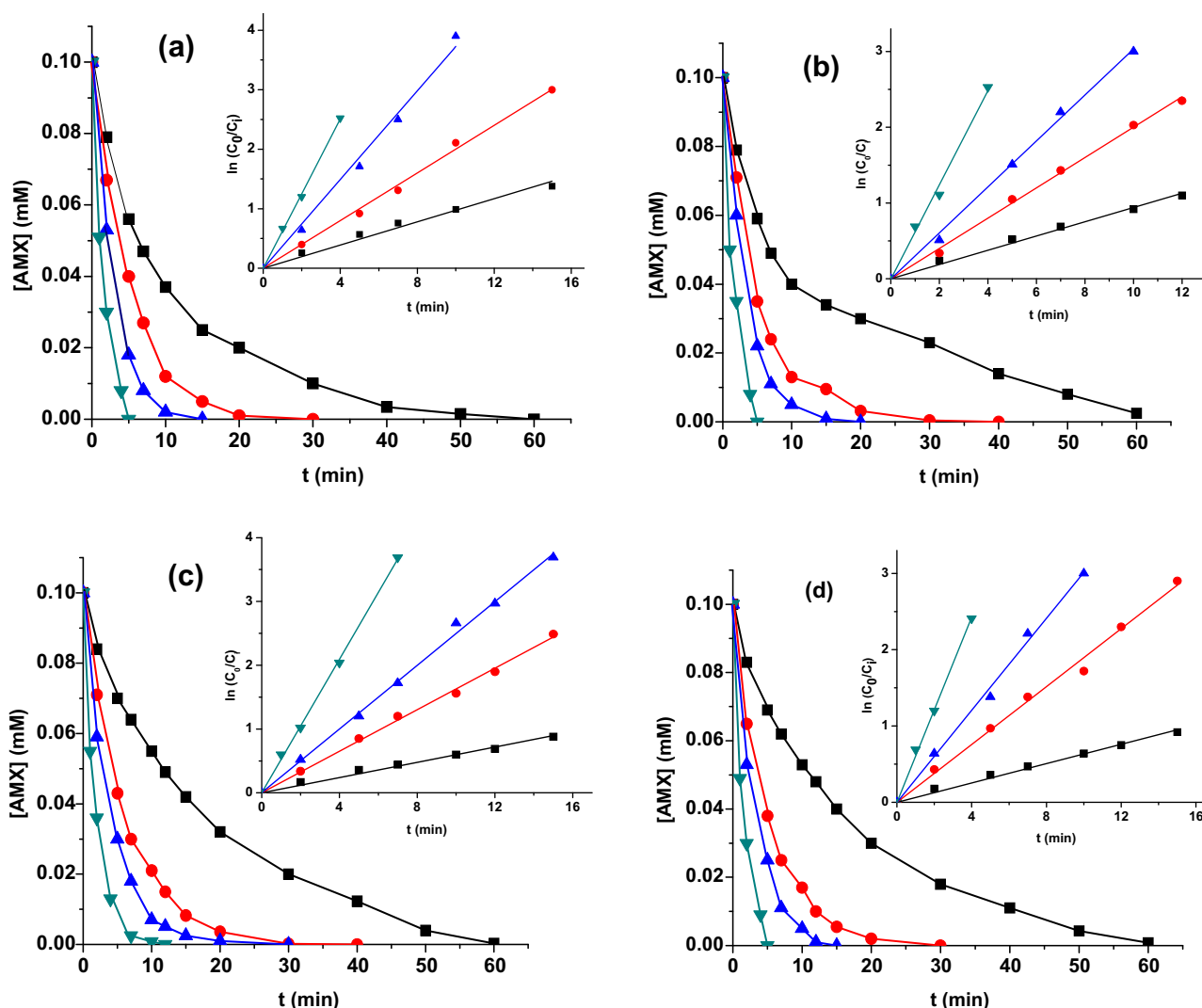
Fig. 1. Effect of applied current: (■) 10 mA, (●) 30 mA, (▲) 60 mA, and (▼) 120 mA on the time-course of AMX concentration decay using (a) Ti_4O_7, (b) BDD (c) DSA and (d) Pt anodes and carbon felt cathode in 0.05 M Na_2O_4. $[AMX]_0 = 0.1$ mM (36.5 mg L^{-1}), $[Fe^{2+}] = 0.1$ mM, V = 230 mL.

as current increases [2,21]. However, enhancement of performance of the anode materials with increased applied current was much significant only at lower applied current values as can be seen in Fig. 2a–d. In fact, application of higher current values above 60 mA showed minimal positive enhancement of TOC removal efficiency, indicating the loss in the relative quantity of •OH/M(•OH) generated owing to the progressive enhancement of wasting reactions that consume hydroxyl radicals without contributing to organic oxidation/mineralization [14,50]. The high current values favor the "self-destruction" of the generated M(•OH) as they are produced in large quantities, especially when treated low-organic content solution as in the case of the present studies.

Besides, comparison of the TOC removal efficiency between AO—H_2O_2 and EF using Ti_4O_7 anode (Fig. 4g) at 5 mA cm^{-2} showed better mineralization with EF compared to AO—H_2O_2 as expected due to contribution of homogeneously generated •OH from Fenton's reaction (Eq. (2)) to the overall degradation of the AMX. Moreover, this result showed the importance of heterogeneously generated M(•OH) in the EF oxidation of organic pollutants when high O_2-overpotential anodes like BDD or Ti_4O_7 are used.

The corresponding MCE values for the trials of Fig. 2a–d are given in (Fig. 3). Similar and excellent MCE values were obtained for both Ti_4O_7 and BDD anodes (Fig. 3a and b) due to the low applied cur-

rents and high TOC removal efficiency obtained for both anodes. For instance, MCE percentages close to 80% were attained for low currents (10 mA) and at early electrolysis times for both Ti_4O_7 and BDD anodes, whereas lower MCE percentages of ∼ 60% were obtained at similar current with DSA or Pt anode, demonstrating higher potential and effectiveness of Ti_4O_7 in EF treatment of organic pollutants. In all cases, MCE < 100% was observed, because •OH/M(•OH) production requires mass transport of reactants and organics on the one hand and involvement of side reactions on the other hand [50]. Evolution of MCE(%) with current exhibits opposite trend compared to TOC removal (i.e. decreases with rise in applied current) regardless of anode materials used. This can be explained by gradual loss in relative quantity of •OH/M(•OH) formed owing to the enhancement of waste reactions (such as consumption of •OH/M(•OH) in the reactions with H_2O_2 and Fe^{2+}) competing with oxidation of AMX that causes the decrease in mineralization of the organics [8,14,50]. High currents can also lead to the energy loss in side reactions like the evolution of H_2 at cathode and O_2 at the anode. Besides, similar slow fall of MCE(%) with time was observed at all experimental condition studied, which can be explained by formation of less easily oxidized intermediates such as short-chain carboxylic acids as well as depletion of pollutant concentration in the treated solution [2,53,54].
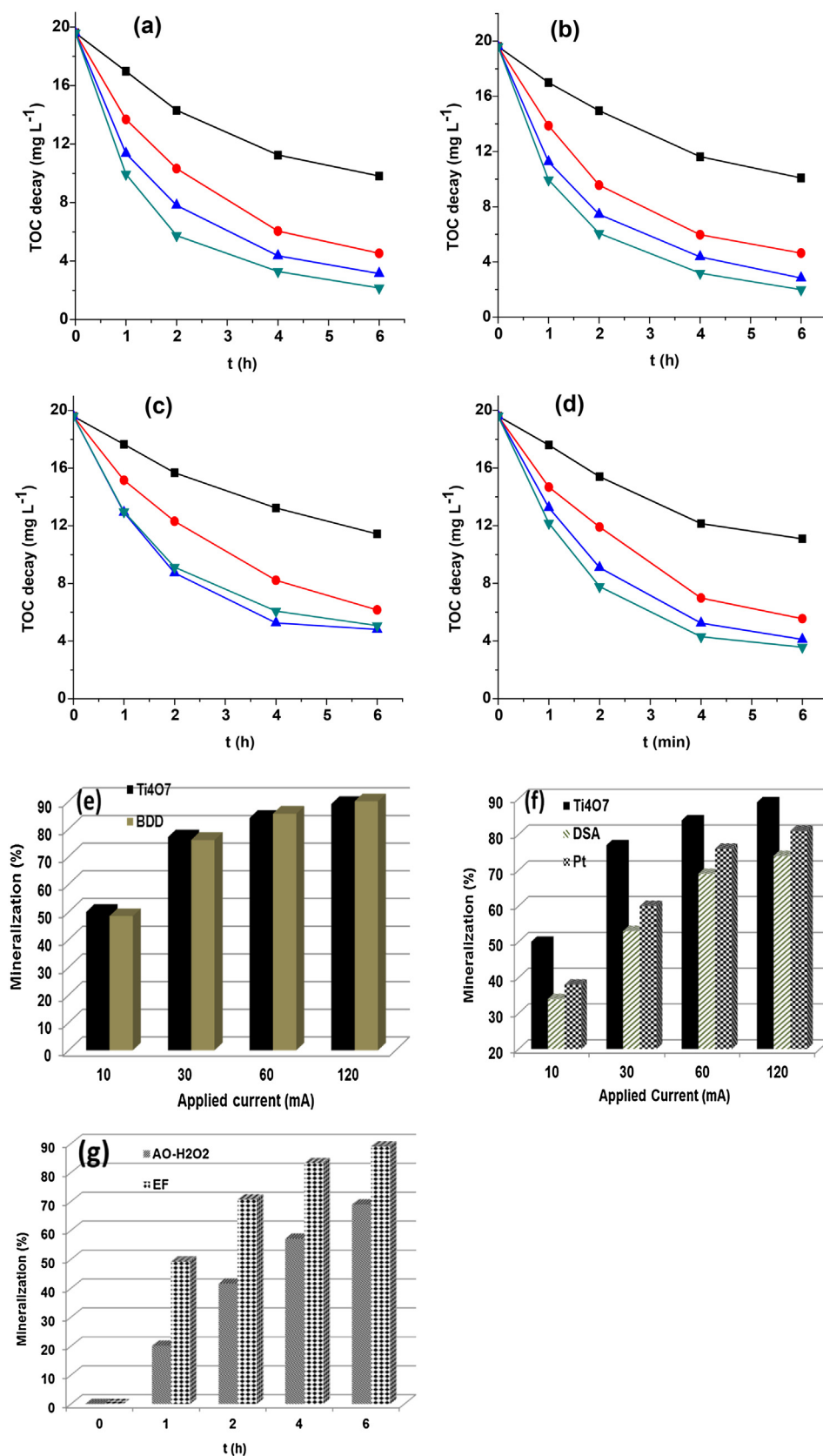
Fig. 2. Effect of applied current on TOC removal efficiency with electrolysis time for the mineralization of 0.1 mM (19.6 mg L^{-1} TOC) AMX solution in 0.05 M Na$_2$O$_4$ and 0.1 mM catalyst (Fe^{2+}) at applied current of (■) 10 mA, (●) 30 mA, (▲) 60 mA, and (▼) 120 mA using (a) Ti$_4$O$_7$, (b) BDD, (c) DSA and (d) Pt anodes. The figure (e) shows the comparison of TOC removal versus applied current between Ti$_4$O$_7$ and BDD anodes, (f) Ti$_4$O$_7$, DSA and Pt after 6 h of electrolysis and (g) AO—H$_2$O$_2$ versus EF using Ti$_4$O$_7$ anode at 120 mA.
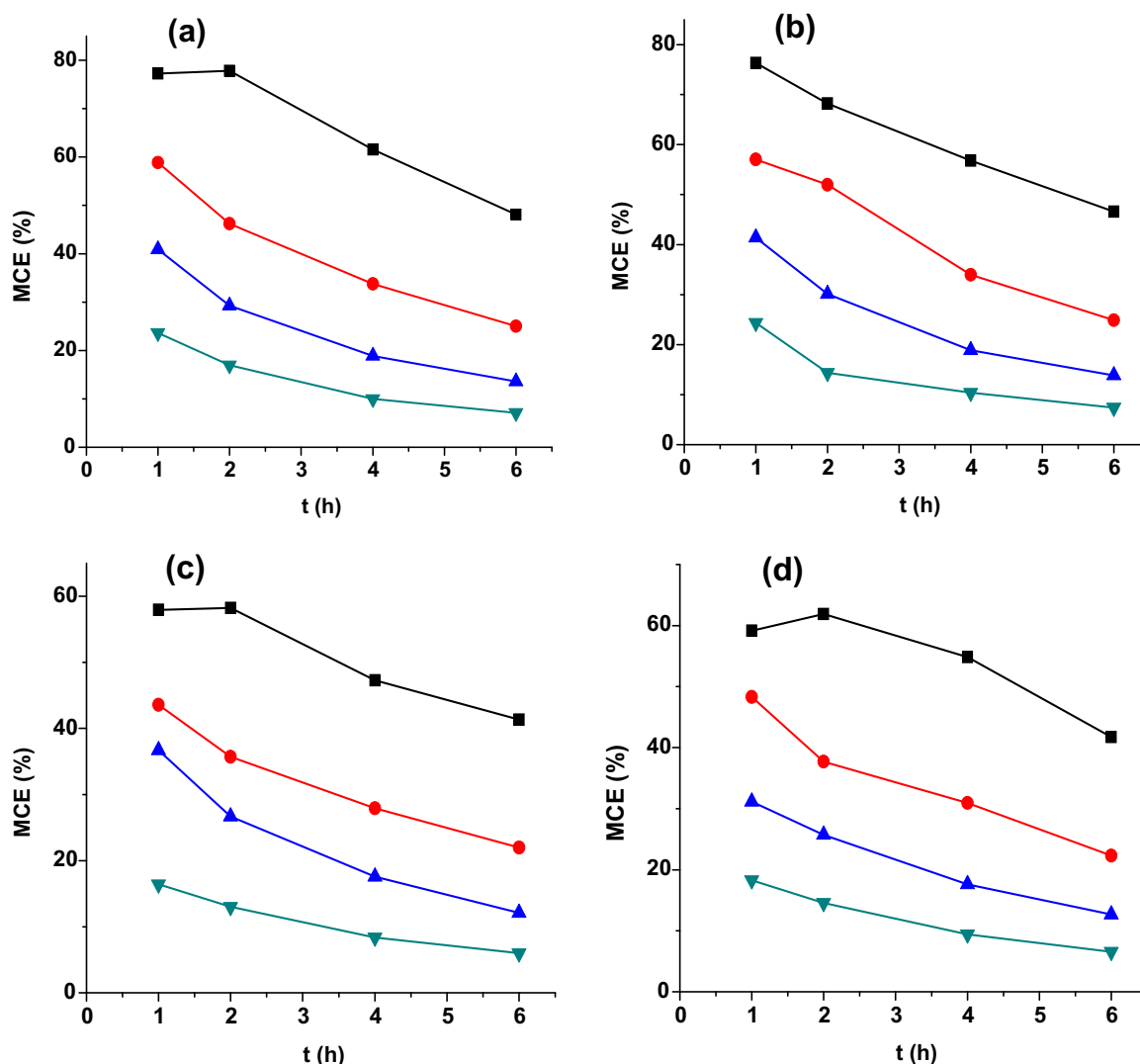
Fig. 3. Evolution of MCE% during electrolysis of 0.1 mM AMX solution by EF process with (a) Ti_4O_7, (b) BDD, (c) DSA and (d) Pt anodes for applied currents of: (■) 10 mA, (●) 30 mA, (▲) 60 mA, and (▼) 120 mA.

The amount of electrical energy consumed per TOC mass (EC_{TOC} in kWh per g TOC removed) is an important parameter for ability of an electrochemical process in industrial level. The EC_{TOC} values for the trials of Fig. 2a–d were determined from Eq. (7) and the results are shown in Fig. 4 [2–4]. This parameter (EC_{TOC}) may constitute an interesting data because it evaluates the energy cost of the process related to TOC removal.

$$EC_{TOC} \left(\text{kWh(g TOC)}^{-1} \right) = \frac{E_{cell} \times I \times \Delta t}{\Delta (TOC) \times V_{sol}} \tag{7}$$

where E_{cell} (volt) is the cell voltage between anode and cathode, I is the applied current (A), Δt is the time (h), $\Delta(TOC)$ is the amount of TOC removed (g carbon L^{-1}) and V_{sol} is the volume of the treated solution (L).

As depicted in Fig. 4, the overall energy cost for mineralization of 0.1 mM AMX solution (corresponding to 19.6 mg L^{-1} TOC) increases as the applied current increases from 10 to 120 mA regardless of the anode material used. For instance, 0.055, 0.121, 0.30 and 0.68 kWh of electrical energy were consumed for g TOC removed after 6 h of electrolysis at 10, 30, 60 and 120 mA, respectively, with Ti_4O_7 anode. This implied that for 6 h of treatment, the energy cost at 10 mA is 12 times lower than that of 120 mA. However, the higher energy cost at high applied current is compen-

sated by the excellent mineralization efficiency. Interestingly, in the cases of Ti_4O_7 and BDD similar amount of electrical energy were consumed after 6 h of treatment at all current studied (Fig. 4a and b). Therefore, it can be concluded that Ti_4O_7 anode is an excellent substitute for BDD anode material in electrochemical wastewater treatment. On the other hand, relatively lower energy cost at all applied current was observed with either DSA or Pt anode compared to values obtained for both Ti_4O_7 and BDD anodes. The industrial DSA and Pt anodes consumed less electrical energy per unit TOC removal (Fig. 4c and d) during electrochemical treatment owing to low cell voltage related to their high electrical conductivity. However, the mineralization efficiency at all current for DSA and Pt anodes was lower compared to Ti_4O_7 or BDD anode, thus reduced the gained in energy cost.

3.3. Evolution of inorganic ions and carboxylic acids during EF degradation of AMX

The complete mineralization of an organic compound containing heteroatoms generally proceeds via formation of organic intermediates especially carboxylic acids, which are further mineralized to CO_2 and the release of inorganic ions [55,56]. While the generated carboxylic acids are the final end organic intermediate
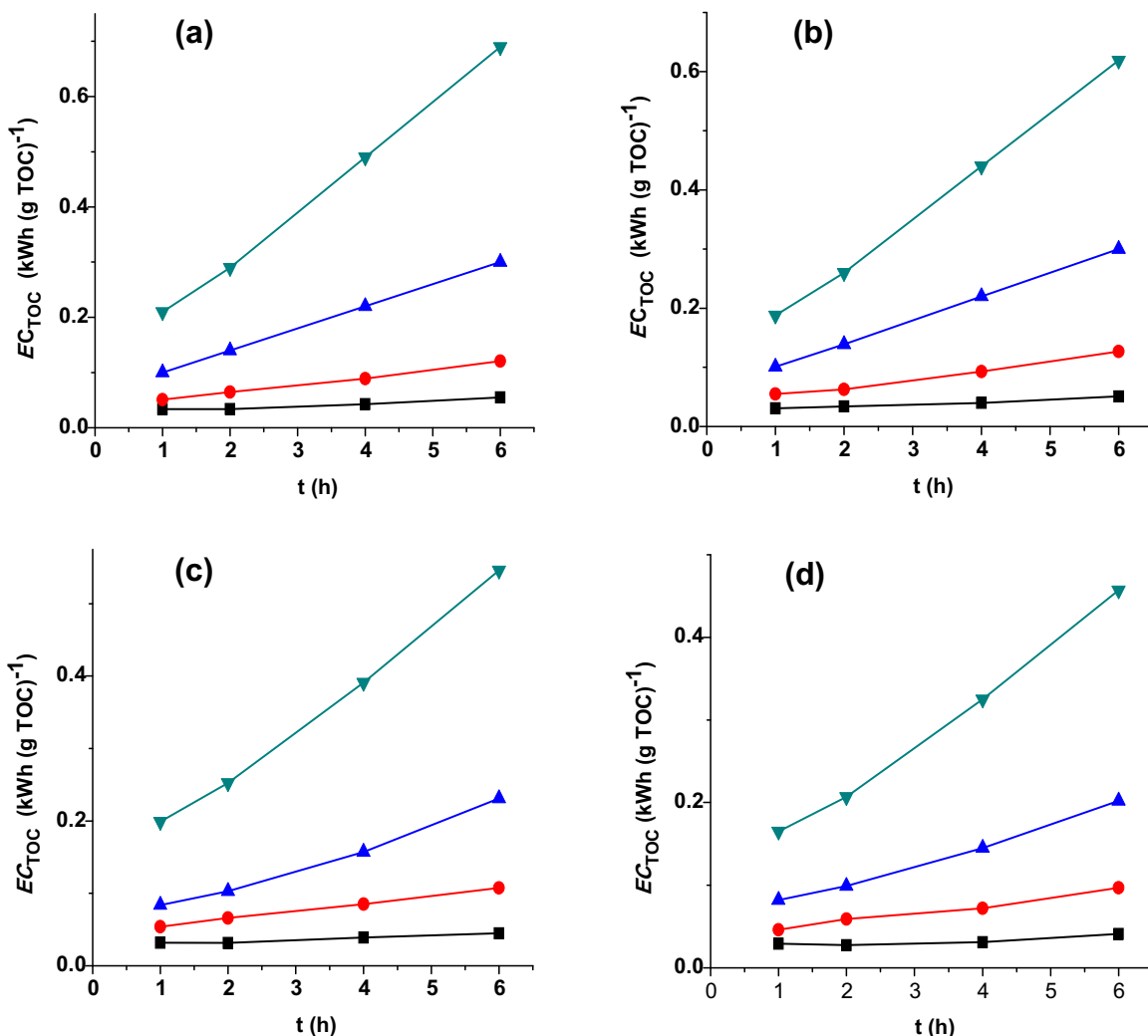
Fig. 4. Evolution of electrical energy consumption per unit TOC mass removed with electrolysis time as a function of applied current: (■) 10 mA, (●) 30 mA, (▲) 60 mA, and (▼) 120 mA for (a) Ti_4O_7, (b) BDD, (c) DSA and (d) Pt anodes.
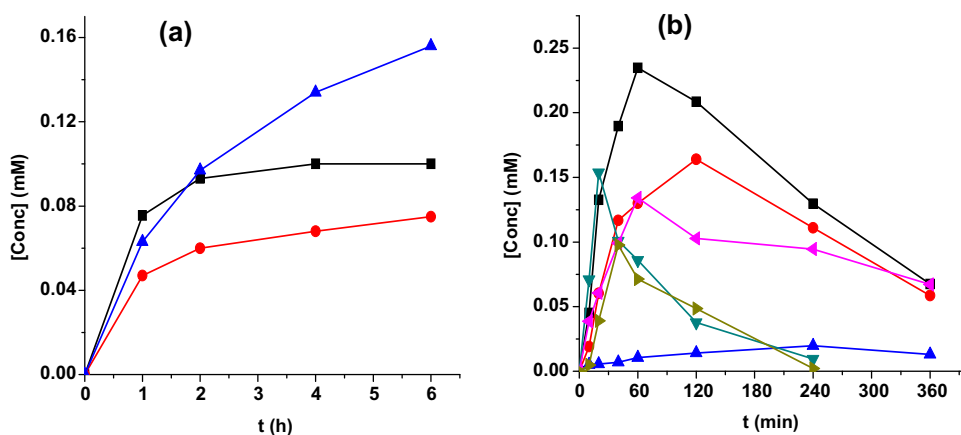
Fig. 5. Evolution of (a) inorganic ions: (■) SO_4^{2-}, (●) NO_3^- and (▲) NH_4^+ and b) short-chain carboxylic acids: (■) oxalic, (●) oxamic, (▲) maleic, (▼) malonic, (◄) acetic, and (►) glycoxylic + during electrolysis of 0.1 mM AMX solution by EF process with Ti_4O_7 anode and carbon-felt cathode at applied current of 120 mA.

by-products of the oxidation of organic pollutants, the release of inorganic ions in the treated solution is another indicator (along with TOC removal degree) of mineralization of organic pollutant under study [53,57–59]. Upon bond cleavage of the AMX molecules, the S atoms were released as SO_4^{2-}, and the N atoms were

recovered in the electrolyzed solution as NH_4^+ and NO_3^- without detecting NO_2^-. The entire S atom (0.1 mM) in 0.1 mM AMX was released as SO_4^{2-} ion and practically accumulated within the first 2 h of electrolysis, indicating that the S bridge in the AMX molecules is a high reacting site for hydroxyl radicals attack on

AMX. The N atoms were majorly recovered as NH_4^+ which continuously accumulated over the electrolysis time, with significant portion released as NO_3^- in the electrolyzed solution mostly at the early hour of the treatment. The continuous increase in NH_4^+ concentration can be related to formation of this ion from reduction of NO_3^- at the cathode, which is in agreement with its study state behavior after 2 h electrolysis. After 6 h of electrolysis, the final treated solution contained 0.1 mM SO_4^{2-} ion (100% of initial S atom), 0.156 mM NH_4^+ ion (52% of initial N) and 0.075 mM NO_3^- ion (25% of initial N). This implies that only 77% of initial N in AMX was released as inorganic N; while the rest was remained partly in the electrolyzed solution as non-mineralized nitrogenous organics, majorly oxamic acid with concentration of 0.058 mM (Fig. 5a) representing ∼19% of the initial N atoms of 0.1 mM AMX.

The ion-exclusion chromatograms of the electrolyzed solution under the conditions of Fig. 2a exhibited well-defined peaks related to oxalic, malonic, oxamic, maleic, glycoxylic and acetic acids at retention time (t_R) of 8.4, 9.6, 12.2, 13.7, 15.2 and 17.1 min, respectively. Maleic, malonic and glycoxylic acids are expected to form from the cleavage of the benzoic ring of the intermediates prior to further oxidation to oxalic acid. Oxamic and acetic acids could be generated from the breaking of lateral chain of AMX molecule. Overall, the concentration profile of all generated acids follows accumulation-destruction cycle with high formation rate at the early stage of the treatment, thanks to the quick oxidation of the AMX and its cyclic intermediates by the electrogenerated hydroxyl radicals, whereas longer treatment time ensure the gradual destruction of the formed carboxylic acid due to generation of large quantities of physisorbed hydroxyl radical ($Ti_4O_7(^•OH)$) which is efficient in mineralization of refractory organics like carboxylic acids. Besides, maleic, malonic and glycoxylic acids were either quickly destroyed or weakly accumulated in electrolyzed solution owing to their further oxidation to oxalic or acetic acid [57,59]. As can been seen in Fig. 5b, oxalic, oxamic and acetic acids were the most accumulated and persisted during the electrolysis, with the concentration of 0.08, 0.06 and 0.07 mM respectively in final solution after 6 h of EF treatment. The presence of these carboxylic acids is accounted for the residual TOC (∼2.0 mg L^{-1}) found in the final solution for the trial performed at 120 mA using Ti_4O_7 anode as reported in Fig. 2a.

Similar reaction pathway has been reported for the oxidation of AMX by $^•$OH [46]. For instance, cyclic/aromatic by-products such as 2-amino (4-hydroxyphenyl) acetic acid, *p*-hydroxybenzoic and several bicyclical lactamic products were detected by GC–MS as primary oxidation products as we previously reported. Further oxidation of these primary by-products yielded secondary by-products like hydroquinone and benzoquinone, which are characteristic by-products of oxidation of aromatics by hydroxyl radicals. The mineralization was accompanied by partial release of organic N and S as NH_4^+, NO_3^- and SO_4^{2-} respectively. Subsequent ring-opening of hydroquinone and benzoquinone and oxidation of byproducts lead to the formation of short-chain carboxylic acids such as oxalic, oxamic, malonic, maleic, acetic and glycoxylic acids which were later oxidized to CO_2 and H_2O as shown in Fig. 5b.

3.4. Assessment of acute toxicity during EF degradation of AMX with Ti_4O_7 anode

The change in acute toxicity of 0.1 mM AMX solution over electrolysis time during EF treatment with Ti_4O_7 anode at 120 mA constant current was investigated by monitoring the bioluminescence inhibition of *V. fischeri* bacteria. As depicted in Fig. 6, AMX solution itself shows relatively low bioluminescence inhibition (i.e., low toxicity), however, the percentage inhibition increased sharply with electrolysis time reaching a maximum of 100% after 60 min of electrolysis, indicating a considerable higher toxicity of
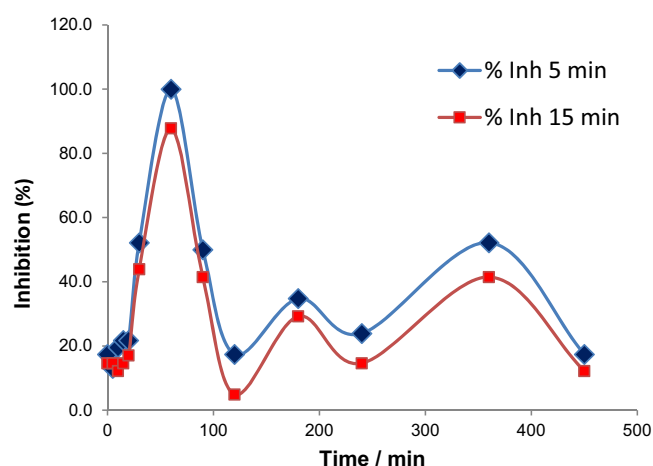

Fig. 6. Evolution of inhibition of luminescence of *Vibrio Fischeri* bacteria as measure of the acute toxicity of 0.1 mM (36.5 mg L^{-1}) AMX solution during EF treatment with Ti_4O_7 anode at 120 mA, after an exposure time of 5 and 15 min.

the primary AMX by-products majorly cyclic and bicyclical lactamic products formed from the cleavage of peptide bond of the initial AMX molecules, which are more toxic than initial AMX molecule. This was followed by sharp decrease, suggesting the toxicity decay due to the oxidation of the primary by-products into less toxic secondary/tertiary intermediates before obtaining a non-toxic final solution at the end of treatment. The formation of more toxic intermediates during AOPs/EAOPs were already reported by our group [48,49]. Besides, similar trend in evolution of toxicity with time has been reported for other antibiotics like sulfachloropyridazine [48], sulfamethoxazole [49] and AMX [46] using BDD anode in either EF or electrooxidation process. It is worth noting that the Ti_4O_7 itself exercises no toxicity effect on the solution, thus making the electrode suitable for wastewater treatment (Fig. 6).

4. Conclusions

The following conclusions can be drawn from the results given and discussed above:

- Ti_4O_7 elaborated by plasma deposition is highly efficient and stable anode material for electro-Fenton oxidation of organic pollutants. Complete degradation and excellent mineralization of AMX was achieved at low current studied. The use of low current is essential in electrochemical process for cost effectiveness of the EAOPs.
- The use of Ti_4O_7 anode in EF process was able to detoxify efficiently 0.1 mM AMX solution, removing completely more toxic intermediates products formed during oxidation of AMX.
- The oxidation ability of this Ti_4O_7 anode for degradation and mineralization of AMX as well as MCE was very similar to that of commercial BDD anode, thus making Ti_4O_7 anode a better alternative for electrochemical advanced oxidation processes due to its low cost of production.
- Comparison studies with industrial electrodes like DSA and Pt showed lower degradation and mineralization rate compared to either Ti_4O_7 or BDD anode.
- The organic S and N atoms in the AMX molecules were released as SO_4^{2-}, NO_3^-, and NH_4^+ and the final end products in the electrolyzed solutions are always inorganic ions and a low residual concentration of short-chain carboxylic acids which are non-toxic and biodegradable compounds.

- Initial AMX solution showed relatively low bioluminescence inhibition to *V. fischeri* bacteria, but sharply increased and decreased with the formation and degradation of intermediates products.
- Based on the obtained results, an optimum electrolysis time of 4 h (2.087 Ah L^{-1} charge) could be appropriate for efficient treatment of AMX solution at 5 mA cm^{-2}. At this electrolysis time, complete destruction of AMX, excellent mineralization of the solution with up to 84% TOC removal, low energy consumption and complete detoxification was achieved with Ti$_4$O$_7$ anode.

Acknowledgement

References

[1] M.A. Rodrigo, N. Oturan, M.A. Oturan, Electrochemically assisted remediation of pesticides in soils and water: A review, Chem. Rev. 114 (2014) 8720–8745.

[2] E. Brillas, I. Sires, M.A. Oturan, Electro-Fenton process and related electrochemical technologies based on Fenton's reaction chemistry, Chem. Rev. 109 (2009) 6570–6631.

[3] M.A. Oturan, J.-J. Aaron, Advanced oxidation processes in water/wastewater treatment: principles and applications. A review, Crit. Rev. Environ. Sci. Technol 44 (2014) 2577–2641.

[4] C.A. Martínez-Huitle, M.A. Rodrigo, I. Sirés, O. Scialdone, Single and coupled electrochemical processes and reactors for the abatement of organic water pollutants: a critical review, Chem. Rev. 115 (2015) 13362–13407.

[5] E. Brillas, C.A. Martínez-Huitle, Decontamination of wastewaters containing synthetic organic dyes by electrochemical methods. An updated review, Appl. Catal. B: Environ. 166–167 (2015) 603–643.

[6] I. Sirés, E. Brillas, Remediation of water pollution caused by pharmaceutical residues based on electrochemical separation and degradation technologies: a review, Environ. Int. 40 (2012) 212–229.

[7] N. Oturan, J. Wu, H. Zhang, V.K. Sharma, M.A. Oturan, Electrocatalytic destruction of the antibiotic tetracycline in aqueous medium by electrochemical advanced oxidation processes: effect of electrode materials, Appl. Catal. B: Environ. 140-141 (2013) 92–97.

[8] F. Sopaj, N. Oturan, J. Pinson, F. Podvorica, M.A. Oturan, Effect of the anode materials on the efficiency of the electro-Fenton process for the mineralization of the antibiotic sulfamethazine, Appl. Catal. B: Environ. 199 (2016) 331–341.

[9] F. Sopaj, M.A. Rodrigo, N. Oturan, F.I. Podvorica, J. Pinson, M.A. Oturan, Influence of the anode materials on the electrochemical oxidation efficiency. Application to oxidative degradation of the pharmaceutical amoxicillin, Chem. Eng. J. 262 (2015) 286–294.

[10] J.H.B. Rocha, M.M.S. Gomes, E.V. dos Santos, E.C.M. de Moura, D.R. da Silva, M.A. Quiroz, C.A. Martínez-Huitle, Electrochemical degradation of Novacron Yellow C-RG using boron-doped diamond and platinum anodes: direct and Indirect oxidation, Electrochim. Acta 140 (2014) 419–426.

[11] M. Panizza, G. Cerisola, Direct and mediated anodic oxidation of organic pollutants, Chem. Rev. 109 (2009) 6541–6569.

[12] M. Panizza, G. Cerisola, Electrochemical degradation of methyl red using BDD and PbO$_2$ anodes, Ind. Eng. Chem. Res. 47 (2008) 6816–6820.

[13] M.A. Quiroz, J.L. Sánchez-Salas, S. Reyna, E.R. Bandala, J.M. Peralta-Hernández, C.A. Martínez-Huitle, Degradation of 1-hydroxy-2,4-dinitrobenzene from aqueous solutions by electrochemical oxidation: role of anodic material, J. Hazard. Mater. 268 (2014) 6–13.

[14] M. Panizza, A. Dirany, I. Sirés, M. Haidar, N. Oturan, M.A. Oturan, Complete mineralization of the antibiotic amoxicillin by electro-Fenton with a BDD anode, J. Appl. Electrochem 44 (2014) 1327–1335.

[15] A.M. Sales Solano, C.K. Costa de Araújo, J. Vieira de Melo, J.M. Peralta-Hernandez, D. Ribeiro da Silva, C.A. Martínez-Huitle, Decontamination of real textile industrial effluent by strong oxidant species electrogenerated on diamond electrode: viability and disadvantages of this electrochemical technology, Appl. Catal. B: Environ. 130–131 (2013) 112–120.

[16] M.A. Oturan, M.C. Edelahi, N. Oturan, K. El kacemi, J.-J. Aaron, Kinetics of oxidative degradation/mineralization pathways of the phenylurea herbicides diuron, monuron and fenuron in water during application of the electro-Fenton process, Appl. Catal. B: Environ. 97 (2010) 82–89.

[17] E. Bocos, N. Oturan, M.A. Sanromán, M.A. Oturan, Elimination of radiocontrast agent Diatrizoic acid from water by electrochemical advanced oxidation: kinetics study, mechanism and mineralization pathway, J. Electroanal. Chem. 777 (2016) 1–8.

[18] L. Zhou, M.H. Zhou, Z.X. Hu, Z.H. Bi, K.G. Serrano, Chemically modified graphite felt as an efficient cathode in electro-Fenton for p-nitrophenol degradation, Electrochim. Acta 140 (2014) 376–383.

[19] J. Wu, H. Zhang, N. Oturan, Y. Wang, L. Chen, M.A. Oturan, Application of response surface methodology to the removal of the antibiotic tetracycline by electrochemical process using carbon-felt cathode and DSA (Ti/RuO2−IrO2) anode, Chemosphere 87 (2012) 614–620.

[20] H. Olvera-Vargas, N. Oturan, E. Brillas, D. Buisson, G. Esposito, M.A. Oturan, Electrochemical advanced oxidation for cold incineration of the pharmaceutical ranitidine: mineralization pathway and toxicity evolution, Chemosphere 117 (2014) 644–651.

[21] N. Oturan, E. Brillas, M.A. Oturan, Unprecedented total mineralization of atrazine and cyanuric acid by anodic oxidation and electro-Fenton with a boron-doped diamond anode, Environ. Chem. Lett. 10 (2012) 165–170.

[22] M. Diagne, V.K. Sharma, N. Oturan, M.A. Oturan, Depollution of indigo dye by anodic oxidation and electro-Fenton using B-doped diamond anode, Environ. Chem. Lett. 12 (2014) 219–224, http://dx.doi.org/10.1007/s10311-013-0437-z.

[23] S. Garcia-Segura, E.B. Cavalcanti, E. Brillas, Mineralization of the antibiotic chloramphenicol by solar photoelectro-Fenton, Appl. Catal. B: Environ. 144 (2014) 588–598.

[24] F.L. Souza, C. Sáez, M.R.V. Lanza, P. Cañizares, M.A. Rodrigo, Removal of pesticide 2, 4-D by conductive-diamond photoelectrochemical oxidation, Appl. Catal. B: Environ. 180 (2016) 733–739.

[25] M.A. Rodrigo, P. Cañizares, C. Buitrón, C. Sáez, Electrochemical technologies for the regeneration of urban wastewaters, Electrochim. Acta 55 (2010) 8160–8164.

[26] D.M. de Araújo, C. Sáez, C.A. Martínez-Huitle, P. Cañizares, M.A. Rodrigo, Influence of mediated processes on the removal of Rhodamine with conductive-diamond electrochemical oxidation, Appl. Catal. B: Environ. 166–167 (2015) 454–459.

[27] I. Sirés, E. Brillas, M.A. Oturan, M.A. Rodrigo, M. Panizza, Electrochemical advanced oxidation processes: today and tomorrow. A review, Environ. Sci. Pollut. Res. 21 (2014) 8336–8367.

[28] S.O. Ganiyu, E.D. van Hullebusch, M. Cretin, G. Esposito, M.A. Oturan, Coupling of membrane filtration and advanced oxidation processes for removal of pharmaceutical residues: a critical review, Sep. Purif. Technol. 156 (2015) 891–914.

[29] B.P. Chaplin, Critical review of electrochemical advanced oxidation processes for water treatment applications, Environ. Sci. Process. Impacts 16 (2014) 1182.

[30] S. Andersson, B. Collén, U. Kuylenstierna, A. Magnéli, A. Magnéli, H. Pestmalis, S. Åsbrink, Phase analysis studies on the titanium-oxygen system, Acta Chem. Scand. 11 (1957) 1641–1652.

[31] F.C. Walsh, R.G.A. Wills, The continuing development of Magnéli phase titanium sub-oxides and Ebonex® electrodes, Electrochim. Acta 55 (2010) 6342–6351.

[32] P. Geng, J. Su, C. Miles, C. Comninellis, G. Chen, Highly-ordered Magnéli Ti$_4$O$_7$ nanotube arrays as effective anodic material for electro-oxidation, Electrochim. Acta 153 (2015) 316–324.

[33] G. Chen, E.A. Betterton, R.G. Arnold, Electrolytic oxidation of trichloroethylene using a ceramic anode, J. Appl. Electrochem. 29 (1999) 961–970.

[34] M. Hirasawa, T. Seto, T. Orii, N. Aya, H. Shimura, Synthesis of size-selected TiOx nanoparticles, Appl. Surf. Sci. 197–198 (197) (2002) –−.

[35] J.R. Smith, F.C. Walsh, R.L. Clarke, Electrodes based on Magneli phase titanium oxides: the properties and applications of Ebonex$^{(R)}$ materials, J. Appl. Electrochem. 28 (1998) 1021–1033.

[36] K. Kolbrecka, J. Przyluski, Sub-stoichiometric titanium oxides as ceramic electrodes for oxygen evolution − structural aspects of the voltammetric behaviour of Ti$_n$O$_{2n-1}$, Electrochim. Acta 39 (1994) 1591–1595.

[37] T. Ioroi, Z. Siroma, N. Fujiwara, S. Yamazaki, K. Yasuda, Sub-stoichiometric titanium oxide-supported platinum electrocatalyst for polymer electrolyte fuel cells, Electrochem. Commun. 7 (2005) 183–188.

[38] C. Tang, D. Zhou, Q. Zhang, Synthesis and characterization of Magneli phases: reduction of TiO$_2$ in a decomposed NH$_3$ atmosphere, Mater. Lett 79 (2012) 42–44.

[39] G. Chen, C.C. Waraksa, H. Cho, D.D. Macdonald, T.E. Mallouka, EIS studies of porous oxygen electrodes with discrete particles, J. Electrochem. Soc. 150 (2003) E423.

[40] A. Kitada, G. Hasegawa, Y. Kobayashi, K. Kanamori, K. Nakanishi, H. Kageyama, Selective preparation of macroporous monoliths of conductive titanium oxides Ti$_n$ O$_{2n-1}$ (n = 2, 3, 4, 6), J. Am. Chem. Soc 134 (2012) 10894–10898.

[41] X. Zhang, Y. Liu, J. Ye, R. Zhu, Fabrication of Ti$_4$O$_7$ electrodes by spark plasma sintering, Mater. Lett. 114 (2014) 34–36.

[42] D. Bejan, E. Guinea, N.J. Bunce, On the nature of the hydroxyl radicals produced at boron-doped diamond and Ebonex® anodes, Electrochim. Acta 69 (2012) 275–281.

[43] A.M. Zaky, B.P. Chaplin, porous substoichiometric TiO$_2$ anodes as reactive electrochemical membranes for water treatment, Environ. Sci. Technol. 47 (2013) 6554–6563.

[44] A.M. Zaky, B.P. Chaplin, Mechanism of p-substituted phenol oxidation at a Ti$_4$O$_7$ reactive electrochemical membrane, Environ. Sci. Technol. 48 (2014) 5857–5867.

[45] D. Bejan, J.D. Malcolm, L. Morrison, N.J. Bunce, Mechanistic investigation of the conductive ceramic Ebonex® as an anode material, Electrochim. Acta 54 (2009) 5548–5556, http://dx.doi.org/10.1016/j.electacta.2009.04.057.

[46] S.O. Ganiyu, N. Oturan, S. Raffy, M. Cretin, R. Esmilaire, E. van Hullebusch, G. Esposito, M.A. Oturan, Sub-stoichiometric titanium oxide (Ti$_4$O$_7$) as a suitable ceramic anode for electrooxidation of organic pollutants: a case study of kinetics, mineralization and toxicity assessment of amoxicillin, Water Res. 106 (2016) 171–181.

[47] H. Lin, J. Wu, N. Oturan, H. Zhang, M.A. Oturan, Degradation of artificial sweetener saccharin in aqueous medium by electrochemically generated hydroxyl radicals, Environ. Sci. Pollut. Res. 23 (2016) 4442–4453.

[48] A. Dirany, I. Sirés, N. Oturan, A. Özcan, M.A. Oturan, Electrochemical treatment of the antibiotic sulfachloropyridazine: kinetics, reaction pathways, and toxicity evolution, Environ. Sci. Technol. 46 (2012) 4074–4082.

[49] A. Dirany, S. Efremova Aaron, N. Oturan, I. Sirés, M.A. Oturan, J.J. Aaron, Study of the toxicity of sulfamethoxazole and its degradation products in water by a bioluminescence method during application of the electro-Fenton treatment, Anal. Bioanal. Chem. 400 (2010) 353–360.

[50] I. Sirés, N. Oturan, M.A. Oturan, Electrochemical degradation of β-blockers. Studies on single and multicomponent synthetic aqueous solutions, Water Res. 44 (2010) 3109–3120.

[51] M. Panizza, G. Cerisola, Electrocatalytic materials for the electrochemical oxidation of synthetic dyes, Appl. Catal. B:Environ. 75 (2007) 95–101.

[52] S. Cotillas, J. Llanos, M.A. Rodrigo, P. Cañizares, Use of carbon felt cathodes for the electrochemical reclamation of urban treated wastewaters, Appl. Catal. B: Environ. 162 (2015) 252–259.

[53] H. Lin, J. Niu, J. Xu, Y. Li, Y. Pan, Electrochemical mineralization of sulfamethoxazole by Ti/SnO2-Sb/Ce-PbO2 anode: kinetics, reaction pathways, and energy cost evolution, Electrochim. Acta 97 (2013) 167–174.

[54] H. Lin, N. Oturan, J. Wu, V.K. Sharma, H. Zhang, M.A. Oturan, Removal of artificial sweetener aspartame from aqueous media by electrochemical advanced oxidation processes, Chemosphere 167 (2017) 220–227.

[55] H. Lin, J. Niu, S. Ding, L. Zhang, Electrochemical degradation of perfluorooctanoic acid (PFOA) by Ti/SnO2–Sb, Ti/SnO2–Sb/PbO2 and Ti/SnO2–Sb/MnO2 anodes, Water Res. 46 (2012) 2281–2289.

[56] Q. Zhuo, S. Deng, B. Yang, J. Huang, B. Wang, T. Zhang, G. Yu, Degradation of perfluorinated compounds on a boron-doped diamond electrode, Electrochim. Acta 77 (2012) 17–22.

[57] M.A. Oturan, M. Pimentel, N. Oturan, I. Sirés, Reaction sequence for the mineralization of the short-chain carboxylic acids usually formed upon cleavage of aromatics during electrochemical Fenton treatment, Electrochim. Acta 54 (2008) 173–182.

[58] E.K. Carter, J. Farrell, Oxidative destruction of perfluorooctane sulfonate using boron-doped diamond film electrodes, Environ. Sci. Technol. 42 (2008) 6111–6115.

[59] S. Garcia-Segura, E. Brillas, Mineralization of the recalcitrant oxalic and oxamic acids by electrochemical advanced oxidation processes using a boron-doped diamond anode, Water Res. 45 (2011) 2975–2984.